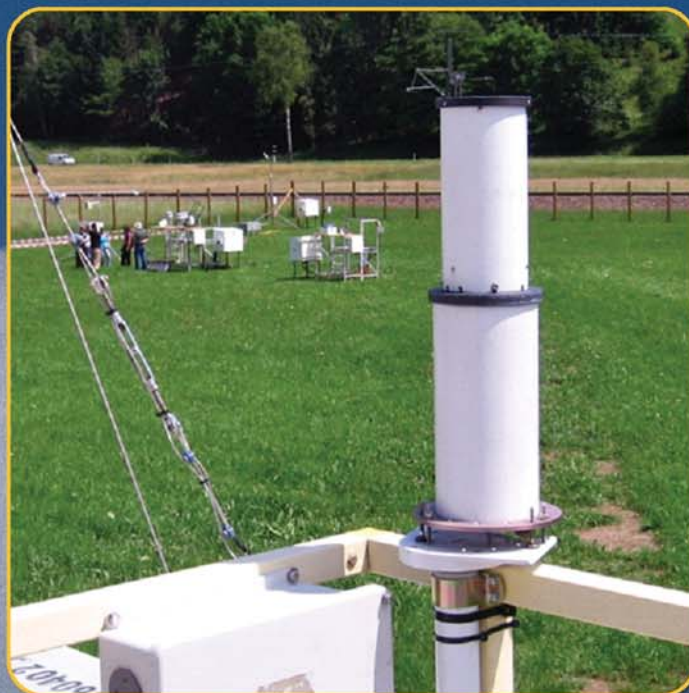
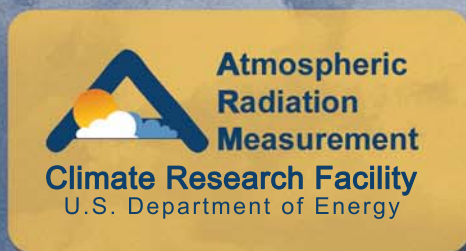


# Narrow Field of View Zenith Radiometer Handbook



November 2008



Work supported by the U.S. Department of Energy  
Office of Science, Office of Biological and Environmental Research

# **Narrow Field of View Radiometer (NFOV) Handbook**

November 2008

C. Chiu  
A. Marshak  
G. Hodges  
J.C. Barnard  
J. Schmelzer

Work supported by the U.S. Department of Energy,  
Office of Science, Office of Biological and Environmental Research

## Contents

1.	General Overview .....	1
2.	Contacts.....	1
	2.1 Mentor.....	1
	2.2 Instrument Developer.....	1
3.	Deployment Locations and History.....	1
4.	Near-Real-Time Data Plots .....	3
5.	Data Description and Examples.....	3
	5.1 Data File Contents.....	3
	5.2 Annotated Examples.....	3
	5.3 User Notes and Known Problems .....	4
	5.4 Frequently Asked Questions .....	4
6.	Data Quality .....	4
	6.1 Data Quality Health and Status .....	5
	6.2 Data Reviews by Instrument Mentor.....	5
	6.3 Data Assessments by Site Scientist/Data Quality Office .....	6
	6.4 Value-Added Procedures and Quality Measurement Experiments .....	6
7.	Instrument Details .....	6
	7.1 Detailed Description.....	6
	7.2 Theory of Operation .....	7
	7.3 Calibration.....	9
	7.4 Operation and Maintenance.....	9
	7.5 Glossary.....	9
	7.6 Acronyms .....	9
8.	Citable References .....	9

## Figures

1.	Downward 870-nm radiances vs. cloud optical depth calculated by the 1D radiative transfer model DISORT with a surface albedo of 0.271.....	2
2.	Downward radiances and normalized radiances of the NFOV2 measured at the Black Forest, Germany, on 15 April 2007 .....	4
3.	The NFOV2 and the enclosure that contains the power supply and data logger. ....	5
4.	A schematic illustration of the REDvsNIR method for retrieving cloud optical depth and cloud fraction. ....	8
5.	A lookup table constructed for SZA = 52°, effective radius of 8 μm, and surface albedo values of 0.13 and 0.28 for RED and NIR channels, respectively. ....	8

## 1. General Overview

The two-channel Narrow Field-of-View Radiometer (NFOV2) is a ground-based radiometer that looks straight up and measures radiance directly above the instrument at wavelengths of 673 and 870 nm. The field-of-view of the instrument is  $1.2^\circ$ , and the sampling time resolution is 1 second. Measurements of the NFOV2 have been used to retrieve optical properties for overhead clouds that range from patchy to overcast. With a 1-sec sampling rate of the NFOV2, faster than almost any other ARM instrument, we are able, for the first time, to capture changes in cloud optical properties at the natural time scale of cloud evolution.

Note that ARM had a one-channel narrow field-of-view (NFOV) radiometer that provided valuable measurements for further developing the NFOV2. More details about NFOV can be found the section 3.

## 2. Contacts

### 2.1 Mentor

Gary Hodges  
Phone: 303-497-6460  
[Gary.Hodges@noaa.gov](mailto:Gary.Hodges@noaa.gov)

Christine Chiu  
Phone: 301-614-6213  
[Christine.Chiu@nasa.gov](mailto:Christine.Chiu@nasa.gov)

### 2.2 Instrument Developer

James Barnard  
Pacific Northwest National Laboratory  
(509) 372-6145  
[james.barnard@pnl.gov](mailto:james.barnard@pnl.gov)

John Schmelzer, Retired

Warren Wiscombe  
Brookhaven National Laboratory  
Phone: (631) 344-4260  
[wwiscomb@bnl.gov](mailto:wwiscomb@bnl.gov)

Alexander Marshak  
Phone: (301) 614-6122  
[Alexander.Marshak@nasa.gov](mailto:Alexander.Marshak@nasa.gov)

## 3. Deployment Locations and History

The narrow field-of-view radiometer was designed as fast (sampling rate of 1 Hz), simple, cheap instrument to measure clouds, and complement the radars, lidars and microwave radiometers by having a similar narrow field of view ( $5.7^\circ$ ). To minimize molecular (Rayleigh) scattering, measurements of the

instrument were taken at a wavelength of 870 nm, and thus the instrument was called 1-channel narrow field-of-view radiometer (NFOV). The NFOV worked well until being damaged during a storm in June 2002, and had been decommissioned since June 2007.

Unlike flux instruments, the NFOV that measures zenith radiance has the potential to provide local estimates of cloud optical depth. But there are two major problems with retrieving cloud optical depth from monochromatic zenith radiance. First, in 1D plane-parallel radiative transfer theory the relationship between solar zenith radiance and cloud optical depth is not a one-to-one function (as shown in Figure 1). Therefore, unambiguously determining the optical depth from radiance measured by a one-channel radiometer is nearly impossible. Second, the histogram of actual observations (solid line in Figure 1) from the NFOV reveals that due to 3D effects, some radiance values may exceed those permitted by 1D models. This results in cloud optical depth being irretrievable for those zenith radiances.

Because of the aforementioned problems, a 2nd channel at 673 nm was added to the new instrument, NFOV2. The NFOV2 was deployed at the SGP site in September 2004. Soon the NFOV2 became one of the main radiometers of the ARM Mobile Facility (AMF) with deployments in June–September 2005 at Point Reyes, CA, and at the Black Forest of Germany in 2007. Currently, the NFOV2 is in China with the AMF for the study of aerosol indirect effects.

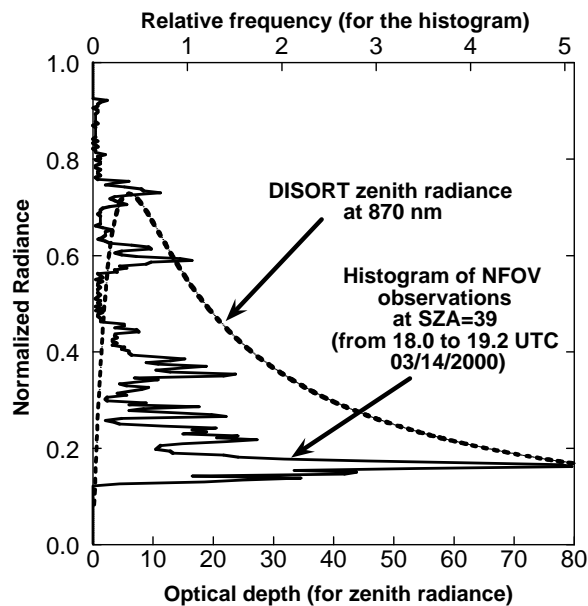


**Figure 1.** Downward 870-nm radiances vs. cloud optical depth (lower x-axis) calculated by the 1D radiative transfer model DISORT (*Stamnes et al.*, 1988) with a surface albedo of 0.271. Co-plotted solid curve is a histogram (upper x-axis) of NFOV 870-nm radiances measured at the ARM Oklahoma site from 18 to 19.2 UTC, March 14, 2000.

When the NFOV2 was deployed at the SGP site, it had the same a field-of-view as NFOV ( $5.7^\circ$ ). However, it has been found that incorrect cloud optical depths would be retrieved when the instrument's FOV was filled with both clouds and clear-sky. To lower the amount of clear-sky contaminations (*Chiu et al.*, 2006), the FOV was then reduced to  $1.2^\circ$ , which had the side benefit of matching the fields of view of both the ARM Shortwave Spectrometer and of the NASA AERONET (Aerosol Robotic Network) sun photometers.

## 4. Near-Real-Time Data Plots

Data plots are available from the [DQ Hands Plot Browser](#) for the mobile facility deployments (FKB and HFE).

## 5. Data Description and Examples

### 5.1 Data File Contents

#### 5.1.1 Primary Variable and Expected Uncertainty

The primary variables measured by NFOV radiometers are the:

- Zenith radiance at 673 nm ( $\text{Wm}^{-2}\text{sr}^{-1}\text{nm}^{-1}$ )
- Zenith radiance at 870 nm ( $\text{Wm}^{-2}\text{sr}^{-1}\text{nm}^{-1}$ )

##### 5.1.1.1 Definition of Uncertainty

##### 5.1.2 Secondary Underlying Variables

Additional Information about variables may be found at ARM [netCDF](#) file header descriptions for the NFOV2.

##### 5.1.3 Diagnostic Variables

##### 5.1.4 Data Quality Flags

##### 5.1.5 Dimension Variables

## 5.2 Annotated Examples

Two examples from the AMF COPS (Convective and Orographically-induced Precipitation Study) experiment are shown in Figure 2: the left panel is for a clear day, and the right panel is for a cloudy day. Total sky images are also shown to display the corresponding cloud fields. Figure 2a and 2d show that due to stronger cloud scattering, observed radiances are much higher on the cloudy day than those on the clear day. For both days, radiances at 673 nm (RED) are larger than those at 870 nm (NIR).

We further normalize zenith radiance measurement  $I_{m,\lambda}$  at wavelength  $\lambda$  using:

$$I_{\lambda} = \frac{\pi \cdot I_{m,\lambda}}{\mu_0 \cdot F_{TOA,\lambda}}, \quad (1.1)$$

where  $I_{\lambda}$  is the normalized zenith radiance;  $F_{TOA,\lambda}$  is the solar irradiance at the top of the atmosphere; and  $\mu_0$  is the cosine of solar zenith angle (SZA). From normalized zenith radiances (Figure 2b and 2e), we clearly see that radiances at NIR are larger than those at RED wavelength for the cloudy day.

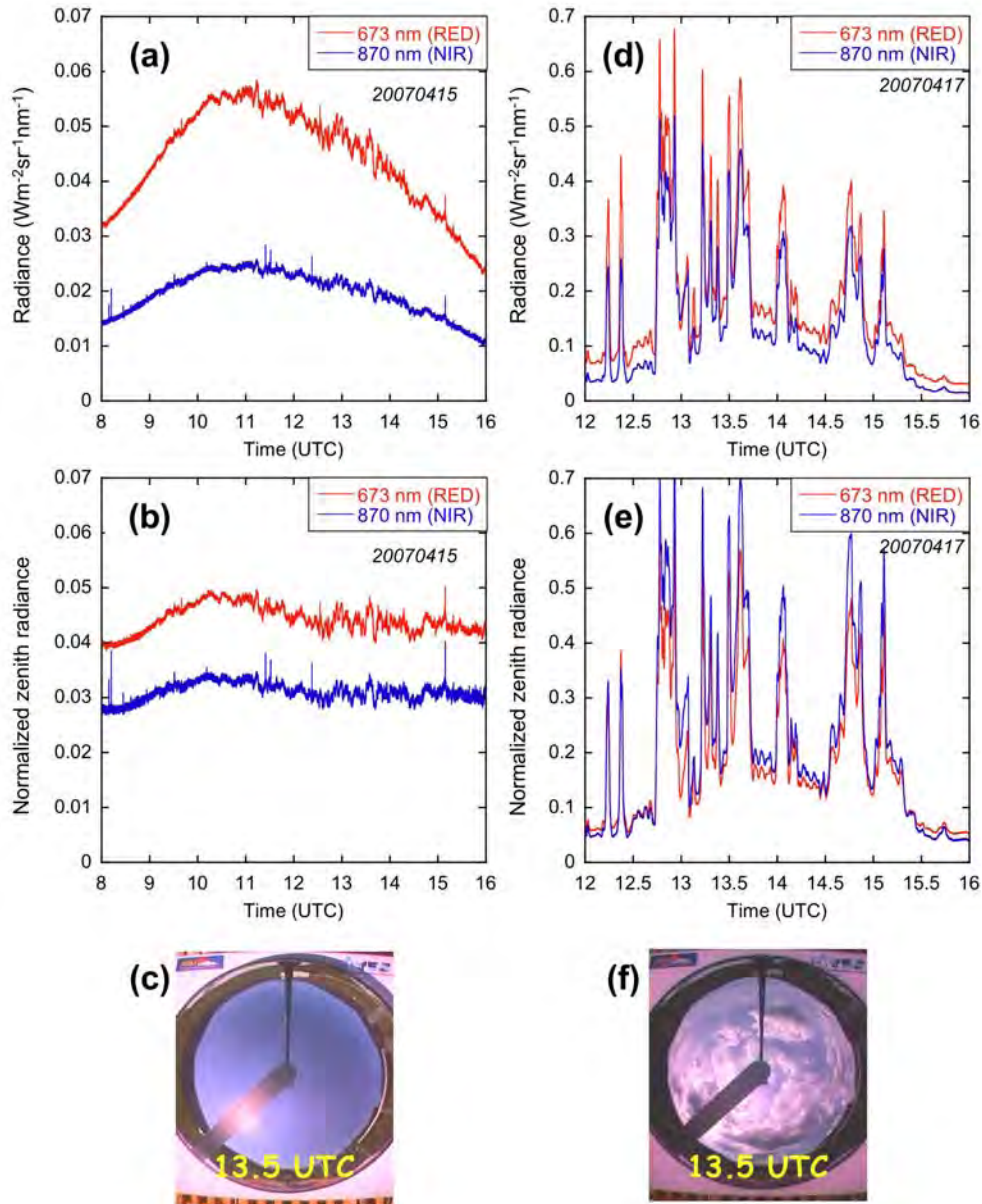


**Figure 2.** Downward radiances (a) and normalized radiances (b) of the NFOV2 measured at the Black Forest, Germany, on 15 April 2007. A total sky image at 13.5 UTC is shown in (c). (d)–(f) are same as (a)–(c), but for 17 April 2007. Note that values of y-axis for these two days are different by an order.

### 5.3 User Notes and Known Problems

### 5.4 Frequently Asked Questions

## 6. Data Quality

Calibrations are performed to produce a calibration factor that converts NFOV2 raw detector counts to zenith radiance. The NFOV2 is calibrated at the NASA Goddard Space Flight Center Calibration Facility, using the 36" integrating Teflon sphere. The sphere, calibrated several times a year using a

spectroradiometer and a secondary lamp standard (<http://cf.gsfc.nasa.gov/docs/proc/radcalprocs.pdf>), has been used to calibrate all sun photometers of the NASA AERONET. Uncertainties in radiances of the sphere at wavelengths of 673 and 870 nm are typically around 1–3 % (<http://cf.gsfc.nasa.gov>).

During the calibration process, dart counts and signals for 4, 8, 12, and 16 lamps of the sphere are measured. A calibration factor is then derived from the relationship between signals of the NFOV2 and radiances of the sphere, using a linear regression approach. A final zenith radiance  $I$  ( $\text{Wm}^{-2}\text{sr}^{-1}\text{nm}^{-1}$ ) is given as

$$I = aV + b, \quad (1.2)$$

where  $a$  is the calibration factor;  $b$  is the offset based on nighttime measurements; and  $V$  is detector counts. Values of  $a$  and  $b$  can be found in the header of data files for both 673 and 870 nm wavelengths.

Note that calibrations are performed when the lens of the NFOV2 is clean. However, in the field, raindrops or other deposits (e.g. sea salt, dust, and bird droppings) might contaminate the lens, which will lead to inaccurate measurements. There are two approaches to correct those measurements. First, one can use linear combinations of calibration factors obtained from the pre- and post- experiment. Second, one can use redundant measurements of the AMF sun photometer. Based on data collected in the AMF COPS deployment, measurements of NFOV2 and the sun photometer agree within 2 %.

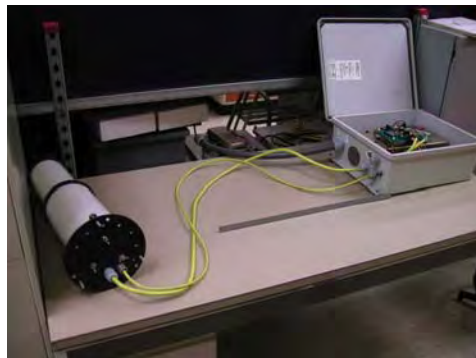


**Figure 3.** The NFOV2 (at left) and the enclosure (at right) that contains the power supply and data logger.

## 6.1 Data Quality Health and Status

The following links go to current data quality health and status results:

- [DQ Hands](#) (Data Quality Health and Status)
- [NCVweb](#) for interactive data plotting using.

The tables and graphs shown contain the techniques used by ARM’s data quality analysts, instrument mentors, and site scientists to monitor and diagnose data quality.

## 6.2 Data Reviews by Instrument Mentor

This section is not applicable to this instrument.



### 6.3 Data Assessments by Site Scientist/Data Quality Office

All DQ Office and most Site Scientist techniques for checking have been incorporated within [DQ HandS](#) and can be viewed there.

### 6.4 Value-Added Procedures and Quality Measurement Experiments

Many of the scientific needs of the ARM Program are met through the analysis and processing of existing data products into “value-added” products or VAPs. Despite extensive instrumentation deployed at the ARM CART sites, there will always be quantities of interest that are either impractical or impossible to measure directly or routinely. Physical models using ARM instrument data as inputs are implemented as VAPs and can help fill some of the unmet measurement needs of the program. Conversely, ARM produces some VAPs not in order to fill unmet measurement needs, but instead to improve the quality of existing measurements. In addition, when more than one measurement is available, ARM also produces “best estimate” VAPs. A special class of VAP called a Quality Measurement Experiment (QME) does not output geophysical parameters of scientific interest. Rather, a QME adds value to the input datastreams by providing for continuous assessment of the quality of the input data based on internal consistency checks, comparisons between independent similar measurements, or comparisons between measurement with modeled results, and so forth. For more information, see the [VAPs and QMEs](#) web page.

## 7. Instrument Details

### 7.1 Detailed Description

#### 7.1.1 List of Components

The instrument consists of two modules, as shown in Figure 3. The instrument on the left is the NFOV2, while the grey enclosure on the right holds the power supply, the head/tube heater controller, and the Campbell data logger. In Figure 3, two yellow cables connect the NFOV2 and the enclosure. The small cable carries current to the window heater, while the large cable carries the signal, and current to heat the head.

Specifications are given as the following:

- Two radiometers:
  - NFOV: 1-channel narrow field-of-view radiometer with a filter 870 nm
  - NFOV2: 2-channel narrow field-of-view radiometer with filters 673 and 870 nm
- Components:
  - The NFOV is comprised of a MFRSR head and a collimator that sits atop the head. The collimator restricts the field of view of the instrument.
- FOV:
  - NFOV: 5.7°
  - NFOV2: 5.7° and 1.2° prior to and after 2004, respectively.
- Bandwidth: 10 nm at full width at half maximum ([response function data](#))

- Detector: Silicon diode detector
- Data output: The data format from the Campbell data logger is:

Column	Descriptions
1	Line number of Campbell code that produces the output
2	Year (e.g., 2008)
3	Julian day
4	Time in HHMM format
5	Time in seconds
6	Output for 870 nm in mV
7	Output for 673 nm in mV
8	Head temperature in mV (this value should be around 1450)
9	Tube temperature in mV (this value should be around 1400)

### 7.1.2 System Configuration and Measurement Methods

### 7.1.3 Specifications

## 7.2 Theory of Operation

The NFOV radiometers point straight up. The collimating tube restricts the FOV of the instruments. The detector that resides in the instrument's head senses photons that travel in the right direction and enter the collimator. The detector is an interference filter/Silicon diode detector. The head is kept at a constant temperature (insofar as possible) to prevent temperature effects from influencing the measurements. The sensitivity to head temperature appears to be about a 1% change in radiance for every 1 K change in head temperature.

### 7.2.1 Retrieval Method for Cloud Optical Properties Theory

Cloud optical depth (or thickness) is a fundamental property for calculating the amount of solar radiation entering and leaving earth's atmosphere. Most techniques to measure this property work well for completely overcast skies, but are inapplicable for broken-cloud skies. *Marshak et al.* (2004) and *Chiu et al.* (2006) developed a retrieval method that uses NFOV2 measurements and works for any 3D cloud situation over a vegetated surface. Their method, dubbed REDvsNIR, works because at 673 nm (RED) and 870 nm (NIR), clouds have nearly identical optical properties while vegetated surfaces reflect quite differently.

The retrieval concept is explained as follows. Consider a plane of normalized zenith radiance at NIR versus that at RED (as shown in Figure 4). For clear-sky situations, due to stronger molecular scattering at shorter wavelengths, radiance at RED is larger than that at NIR wavelengths. Therefore, points below the diagonal in Figure 4 correspond to clear sky. On the contrary, for cloudy situations, radiance at NIR is larger than that at RED wavelengths. The contrast is resulted from stronger surface-cloud interactions at NIR, because vegetated surfaces are bright at NIR wavelengths but dark at red wavelengths. Therefore, points above the diagonal correspond to cloudy situations.

Let us take a look at data points A and B – both are above the diagonal line, indicating they correspond to cloudy situations. They have the same RED radiances and thus have the same cloud optical depths. However, they have different radiances at NIR wavelength. A higher radiance at NIR indicates that more surface-cloud interactions occur and more photons reach the ground. It implies that point B has a smaller cloud fraction than point A. As a result, this method retrieves not only cloud optical depth, but also effective cloud fraction.

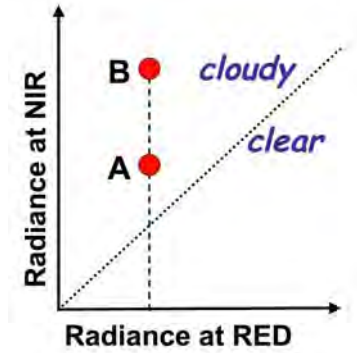


**Figure 4.** A schematic illustration of the REDvsNIR method for retrieving cloud optical depth and cloud fraction.

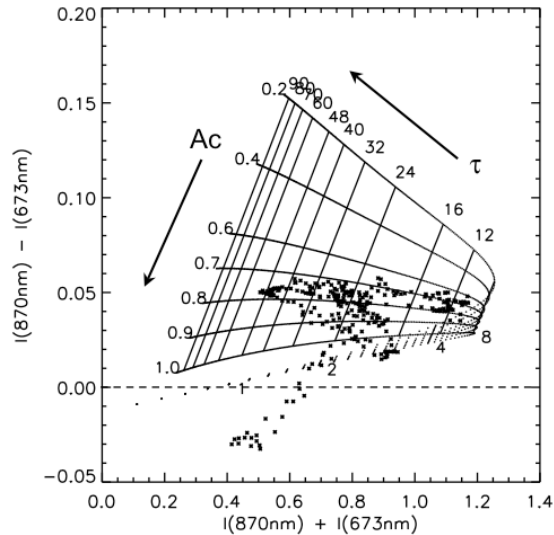


**Figure 5.** A lookup table (lines) constructed for SZA = 52°, effective radius of 8 μm, and surface albedo values of 0.13 and 0.28 for RED and NIR channels, respectively. Dots are normalized zenith radiance measurements from the ARM NFOV2 radiometer at the Oklahoma site during 17.2 and 17.28 UTC on Oct. 28, 2004.  $\tau$  is cloud optical depth and  $A_c$  is effective cloud fraction.

The above illustrations can all be made quantitative in the RED vs NIR method, which retrieves both optical depth  $\tau$  and effective cloud fraction  $A_c$  from a point in the RED vs. NIR plane. We use DISORT (Discrete-Ordinate-method) radiative transfer model to calculate zenith radiance  $I$  over a reasonable range of  $\tau$  and  $A_c$  for both channels, given as

$$\begin{aligned} I_{RED} &= I_{RED}(\tau, A_C) \\ I_{NIR} &= I_{NIR}(\tau, A_C) \end{aligned} \tag{1.3}$$

We then build a 2D lookup table based on these calculations. By plotting radiance measurements on the lookup table (as shown in Figure 5), cloud optical depth and effective cloud fraction can be both determined by the underlying lines. Detailed explanations, sensitivity analyses, and discussions about this retrieval method can be found in *Marshak et al.* (2004) and *Chiu et al.* (2006).

## 7.3 Calibration

### 7.3.1 Theory

### 7.3.2 Procedures

### 7.3.3 History

## 7.4 Operation and Maintenance

### 7.4.1 User Manual

### 7.4.2 Routine and Corrective Maintenance Documentation

### 7.4.3 Software Documentation

### 7.4.4 Additional Documentation

## 7.5 Glossary

See [ARM Glossary](#)

## 7.6 Acronyms

See the [ARM Acronyms and Abbreviations](#)

## 8. Citable References

Chiu, JC, A Marshak, Y Knyazikhin, WJ Wiscombe, HW Barker, JC Barnard, and Y Luo. 2006. "Remote sensing of cloud properties using ground-based measurements of zenith radiance." *Journal of Geophysical Research* 111: D16201, doi:10.1029/2005JD006843.

Marshak, A, Y Knyazikhin, KD Evans, and WJ Wiscombe. 2004. "The 'RED versus NIR' plane to retrieve broken-cloud optical depth from ground-based measurements, Cloud-vegetation interaction: Use of normalized difference cloud index for estimation of cloud optical thickness." *Journal of Atmospheric Science* 61: 1911-1925.

Stamnes, K, S-C Tsay, WJ Wiscombe, and K Jayaweera. 1988. "Numerically stable algorithm for discrete-ordinate-method radiative transfer in multiple scattering and emitting layered media." *Applied Optics* 27: 2502-2512.